Muscle coordination patterns in regulation of medial gastrocnemius activation during walking

Kibushi, Benio

(Citation)
Human Movement Science, 90:103116

(Issue Date)
2023-08

(Resource Type)
journal article

(Version)
Accepted Manuscript

Title: Muscle coordination patterns in regulation of medial gastrocnemius activation during walking

Author: Benio Kibushi[1]*

Author Affiliations:

[1] Graduate School of Human Development and Environment, Kobe University, 3-11 Tsurukabuto, Nada, Kobe, JAPAN

Corresponding Author: Benio Kibushi, Ph. D.

E-mail: kibushi.b@ruby.kobe-u.ac.jp

Word counts: ***3864***

ORCID: https://orcid.org/0000-0001-7015-1806 (Benio Kibushi)

Conflict of interest statement

The author declares no competing financial interests.

Key words:

Muscle synergies, motor module, biofeedback, kinematics, electromyogram

Abstract

The ankle plantar flexion in the late stance phase is referred to as the ankle push-off. When the ankle push-off force is enhanced, compensatory adjustments occur in the adjacent phases. The muscle control that achieves these compensatory movements remains unknown, although they are expected to be coordinately regulated across multiple muscles and phases. Muscle synergy is used as a quantification technique for muscle coordination, and this analysis enables the comparison of synchronized activity between multiple muscles. Therefore, this study aimed to elucidate the tuning of muscle synergies in muscle activation adjustment of push-off. It is hypothesized that muscle activation adjustment of push-off is performed in the muscle synergy related to ankle push-off and in the muscle synergy that activates during the adjacent push-off phase. Eleven healthy men participated, and participants manipulated the activity of the medial gastrocnemius during walking through visual feedback. Two conditions were compared as experimental conditions: increasing the muscle activity to 1.6 times that during normal walking (High) and matching it with that during normal walking (Normal). Twelve muscle activities in the trunk and lower limb and kinematic data were recorded. Muscle synergies were extracted by the non-negative matrix factorization. No significant difference was observed in the number of synergies (High: 3.5 ± 0.8, Normal: 3.7 ± 0.9, $p = 0.21$) and muscle synergy activation timing and duration between the High and Normal conditions ($p > 0.27$). However, significant differences were observed in the peak muscle activity during the late stance phase of the rectus femoris (RF), biceps femoris (BF) between conditions (RF at High: 0.32 ± 0.21, RF at Normal: 0.45 ± 0.17, $p = 0.02$; BF at High: 0.16 ± 0.01, BF at Normal: 0.08 ± 0.06 $p = 0.02$). Although the quantification of force exertion has not been conducted, the modulation of RF and BF activation could have occurred due to the attempts to help knee flexion. Muscle synergies during normal walking are

therefore maintained, and slight adjustments in the amplitude of muscle activity occurred for each muscle.

Introduction

The ankle plantar flexion in the late stance phase is referred to as the ankle push-off and generates propulsion force during walking (Zelik & Adamczyk, 2016). Specifically, the push-off force accelerates the center of mass and allows for the leg swing. The ankle push-off force is recognized to decrease in elderly individuals, and a correlation between the reduction of ankle push-off force and the decline in walking velocity has been suggested (DeVita & Hortobagyi, 2000; Kerrigan et al., 1998). Research on the mechanisms of enhancing ankle push-off force can provide valuable insights into maintaining and improving gait ability.

Adjustment of push-off force in healthy individuals can be achieved even without biofeedback (Lewis & Ferris, 2008), although utilizing biofeedback would accelerate learning. Biofeedback has been demonstrated to improve gait and push-off capability. For instance, the electromyogram (EMG) biofeedback in rehabilitation enhanced walking speed and stride length of walking in patients with stroke or in children with cerebral palsy (Aiello et al., 2005; Colborne et al., 1994; Dursun et al., 2009; Jonsdottir et al., 2007). The biofeedback of the angle between the leading and trailing legs helps increase stride length (Liu et al., 2021). In particular, the biofeedback of the propulsive ground reaction force may be the most effective in increasing push-off force (Franz et al., 2014). Franz et al. (2014) compared the EMG biofeedback of the medial gastrocnemius and the biofeedback of the propulsive ground reaction force and found that the latter was more effective in increasing the propulsive force (Franz et al., 2014). However, the daily use of expensive force plates is impractical, and more convenient methods are required. Inexpensive EMG measurement systems have recently been developed, and EMG biofeedback can be expected to be used as a more accessible approach.

While EMG-BF has been reported not to contribute to the enhancement of ankle plantar flexion force during the push-off phase in healthy elderly individuals (Franz et al., 2014), a study focusing on children with cerebral palsy reported an improvement in ankle plantar flexion force through EMG-BF (Colborne et al., 1994). Consequently, results are inconsistent on whether EMG-BF can enhance the ankle plantar flexion force during push-off. The possibility that EMG-BF enhances the ankle plantar flexion force during push-off in healthy individuals might depend on their walking speeds. As walking speed increases, the gastrocnemius activation also increases, yet the peak propulsive force declined at 120% of preferred speed (Neptune & Sasaki, 2005). Therefore, during high-speed walking, an enhanced gastrocnemius activation might not necessarily result in an enhancement of propulsive force. Nevertheless, the gastrocnemius contributes significantly to propulsive force during gait (Clark et al., 2021). Accordingly, insights concerning the regulation of gastrocnemius muscle activity during the push-off phase are beneficial for understanding the mechanisms of muscular control for the push-off at slow or normal walking speed.

The regulation of ankle push-off force can also impact the regulation at other joints and walking subtasks. Strong ankle push-off is known to produce compensatory movements at the hip joint, and specifically a decrease in peak torque during hip extension and flexion (Lewis & Ferris, 2008) as well as a reduction in anterior hip force (Lewis & Garibay, 2015). The potential for regulation in walking subtasks other than push-off can be inferred from the elderly gait. Weakening of ankle push-off force in the elderly has been reported to cause either an increase in the peak power of the hip flexor muscle at the beginning of stance or of the hip extensor muscle at the late stance as compensation (McGibbon & Krebs, 2004). Thus, compensatory adjustments occur during the ankle push-off phase and in the adjacent phases. However, the muscle control that achieves these compensatory movements remains unknown, although they are expected to be coordinately regulated across multiple muscles and phases, and quantifying muscle coordination is therefore necessary.

Muscle synergy is used as a quantification technique for muscle coordination (Ivanenko et al., 2004; Tresch et al., 1999), and this analysis enables comparison of synchronized activity between multiple muscles. In walking, four to five muscle synergies are extracted, and the function of each muscle synergy is related to the walking subtasks, such as the loading response and propulsion (Ivanenko et al., 2004; Neptune et al., 2009). Muscle synergies during walking remain consistent providing the walking speed and the combination of stride length and stride time do not significantly change (Kibushi et al., 2018, 2022). The number of synergies can be maintained even when the exoskeleton enhances the ankle plantar flexion (Jacobs et al., 2018). Thus, muscle synergies during walking are expected to remain consistent, even with enhanced muscle activation of push-off. However, adjustments to muscle synergy activity patterns are seen when the walking speed is high (Kibushi et al., 2018) or when the stride length is extremely wide or narrow (Kibushi et al., 2022). Therefore, the muscle activation adjustment of push-off during gait may be achieved by fine-tuning muscle synergy activity patterns.

This study aimed to elucidate the tuning of muscle synergies in muscle activation adjustment of push-off. The compensatory adjustments occur both during the ankle push-off phase and in the adjacent phases (Lewis & Ferris, 2008; McGibbon & Krebs, 2004). Therefore, I hypothesized that muscle activation adjustment of push-off is performed in the muscle synergy related to ankle push-off and in the muscle synergy that activates during the adjacent push-off phase.

Methods

Participants

Sample size was estimated using the maximum ankle plantarflexion angle data previously reported using experimental tasks that subjects adjusted for push-off force (Lewis & Ferris, 2008). The effect size (Cohen's *d*) was 0.94, and a priori power analysis based on a paired *t*-test indicated that 11 participants would provide a statistical power of 0.80 at the α level of 0.05 to detect a significant difference. Therefore, 11 healthy men were enrolled (age: 25 ± 3 years, height: 171 ± 2 cm, weight: 66 ± 4 kg [average ± standard deviation]); participants had no muscular or neurological disorders. Written informed consent to participate in the study was provided by the participants after they received a detailed explanation of the purpose of the study and the potential benefits and risks associated with participation. Experimental procedures were conducted in accordance with the Declaration of Helsinki and were approved by the Local Ethics Committee of the Faculty of the Graduate School of Human Development and Environment at Kobe University (approval number: 610-2).

Data collection

To measure kinematic data, reflective markers were attached to 24 anatomical landmarks over the whole body. The position coordinate values were measured using a three-dimensional motion capture system with 12 cameras (OptiTrack Flex 3, NaturalPoint, Inc., Corvallis, OR, USA) operating at 100 Hz. A one gait cycle was defined as right heel contact to the next heel contact.

EMG data of the following muscles in the right lower limb and trunk were recorded for the gastrocnemius medialis (MG), soleus (SOL), tibialis anterior (TA), vastus lateralis (VL), rectus femoris (RF), biceps femoris (BF), semitendinosus (ST), tensor fasciae latae (TFL), gluteus medius (Gmed), gluteus maximus (Gmax), erector spinae at L5 (ES), and abdominal external oblique (EO). Active bipolar electrodes (SX230-1000, Biometrics, Gwent, UK) were placed according to recommendations from the SENIAM project (seniam.org). The electrode distance, length, width and thickness of the electrodes were 20, 37, 20 and 6 mm respectively. EMG signals were amplified, and bandpass filtered between 20 and 450 Hz. Electrical signals were recorded at a sampling frequency of 1,000 Hz and stored on the hard disk of a personal computer using an analog-to-digital converter (cDAQ-9179, National Instruments, Austin, TX, USA).

Experimental setup

Participants manipulated the activity of the MG during walking through visual feedback. Movement and muscle activity were measured, and the joint angles, angular velocities, amplitudes of muscle activity, and muscle synergies compared. The MG was targeted as the feedback among the triceps surae muscles due to the least individual difference in activity confirmed in preliminary experiments. Furthermore, MG has been reported to contribute more to propulsive force than SOL (Clark et al., 2021).

Experiments were conducted in the following sequence: adaptation to treadmill walking, measurement of average muscle activity during normal walking, practice of each experimental condition, and measurement for each experimental condition. The walking speed during the experiments was 4.5 km/h, with a stride time of one second, and the participants walked with their arms crossed and facing forward.

The adaptation to treadmill walking with a metronome was performed for two minutes. After training, the right heel contact timing and the MG activity were measured to calculate the ensemble average of the MG during walking, and the analysis used 30 cycles 80 s after measurement had started. To provide visual feedback of MG activity, real-time rectification, smoothing by the moving average, and normalization of amplitude were performed on the measured MG data. The current waveform was displayed in yellow, and the target waveform was represented by white lines. The current waveform was updated every cycle. Three conditions were set as experimental conditions: increasing the MG activity to 1.6 times that during normal walking (High), reducing it to 0.4 times (Low), and matching it with that during normal walking (Normal). The participants adjusted the current waveform with the target waveform displayed on a monitor located 1.5 m ahead (Fig. 1). Participants practiced each experimental condition in two sets of three min. A rest of 1–2 min was set between conditions. During the measurement of the experimental conditions, the participants walked for two min under each condition, and the analysis was performed over 30 cycles 80 s after measurement had started. The Low condition was excluded from the analysis because half of the participants could not appropriately reduce the

MG activity.

Analysis of gait parameters, joint angle, and angular velocity

To reduce noise, the obtained position coordinate data were applied to a low-pass filter (zero lag fourth-order Butterworth filter, cutoff frequency: 3–19 Hz) based on the cut-off frequency determined by residual analysis. Walking parameters (stride length, stride time, stance time, swing time, and double support time) were calculated based on the timing of heel strike and toe-off. To analyze joint angles, the hip, knee, and ankle joint centers were estimated from the measured position coordinate data. Joint angular velocity was calculated using the first derivative of the joint angle. The maximum values of joint angles and angular velocities in the latter half of the stance phase (30%–60% of gait cycle) were calculated for: ankle plantarflexion angle ($P_{Ank-plant-deg}^{Late-stance}$), ankle plantarflexion velocity ($P_{Ank-plant-vel}^{Late-stance}$), and hip flexion velocity ($P_{Hip-flex-vel}^{Late-stance}$).

EMG procedures and analysis

EMG signals were high-pass filtered (20 Hz) with a zero lag fourth-order Butterworth filter to remove noise. Thereafter, EMG signals were demeaned, digitally rectified, and low-pass filtered at 10 Hz with a zero lag fourth-order Butterworth filter. Low-pass filtered EMG signals were time interpolated over one gait cycle to fit a normalized 201-point time base. Using these procedures, a 12 muscle × 30 gait cycle-sized matrix (12 muscles × 6,030 time steps) was provided for each participant. The EMG matrix was normalized to the peak activity of each EMG signal across conditions (Torres-Oviedo & Ting, 2007). This EMG matrix was used for extracting muscle synergies. The maximum values of normalized EMG amplitude in the latter half of the stance phase (30%–60% of gait cycle) were calculated for: MG ($P_{MG}^{Late-stance}$), RF ($P_{RF}^{Late-stance}$), and BF ($P_{BF}^{Late-stance}$).

Muscle synergy analysis

Muscle synergies were extracted using a non-negative matrix factorization (NMF) algorithm (Lee & Seung, 1999; Torres-Oviedo et al., 2006; Tresch et al., 1999). Each muscle synergy is represented as a time-invariant component that coactivates multiple muscles and is activated by a temporal waveform. The NMF decomposes a matrix into two non-negative matrixes approximately by minimizing the error between the original matrix and a reconstructed matrix. Here, two non-negative matrixes correspond to the weighting and activation of synergies, respectively. The muscle activation pattern for a condition ($\boldsymbol{M}$) is represented by the following equation:

$$\boldsymbol{M} = \sum_{i=1}^{N} \boldsymbol{w_i}\,\boldsymbol{c_i} + \boldsymbol{\varepsilon} \qquad \boldsymbol{w_i} \geq \boldsymbol{0} \quad \boldsymbol{c_i} \geq \boldsymbol{0}$$

where $\boldsymbol{N}$ is the number of synergies, $\boldsymbol{w_i}$ is the weighting of a muscle in a muscle synergy i, $\boldsymbol{c_i}$ denotes an activation that involves a relative contribution of the muscle synergy, and $\boldsymbol{\varepsilon}$ is the residual. The composition of the muscle synergy $\boldsymbol{w_i}$ does not change within a condition, whereas the activation $\boldsymbol{c_i}$ does.

The variability accounted for (VAF) was calculated as an indication of the goodness of fit (Hug et al., 2010; Torres-Oviedo & Ting, 2007) as: 100 × the coefficient of determination from the uncentered Pearson correlation coefficient, which was performed for the entire dataset for every participant (Hug et al., 2010; Torres-Oviedo & Ting, 2007). The number of synergies for each dataset was defined as the minimum number of synergies where the lower bound of the 95% confidence interval exceeded 90% of the VAF (Barroso et al., 2014; Sawers et al., 2015).

The muscle synergies of all conditions and participants were classified using the MATLAB function (kmeans). Based on result of number of synergies, the number of clusters set to four. The classification results depend on the initial values, and classification was consequently repeated 100 times by changing the initial values; the classification results with the minimum sum of distances between each point and the centroid in the cluster were adopted (Esmaeili et al., 2022). The similarity between muscle synergies was evaluated by cosine similarity (r) (Cheung et al., 2005).

The center of activity (CoA) and full width at half maximum (FWHM) in the activation of muscle synergy was calculated per gait cycle. The CoA was quantified as the angle of the vector that pointed to the center of mass of that circular distribution. The CoA was calculated using:

$$A = \sum_{t=1}^{N} (cos\theta_t \times Act_t)$$

$$B = \sum_{t=1}^{N} (sin\theta_t \times Act_t)$$

$$CoA = tan^{-1}(B/A)$$

where θ_t is an angle at a t point (1–201 points) that transformed the gait cycle (1%–100%) into the angle θ (1.79°–360°). Act_t is the activation amplitude of muscle synergy at t. The CoA was calculated in polar coordinates as the inverse tangent of B/A. The FWHM was calculated as the sum of the durations of the intervals where the activation of muscle synergies exceeded half of their maximum (Cappellini et al., 2006; Santuz et al., 2018).

Statistics

Gait parameters, peak values of joint angles and angular velocities, and peak values of muscle activity, CoA, and FWHM were calculated for each participant and each gait cycle and averaged across the gait cycles. The normality of the data was verified using the Shapiro–Wilk test. After the normal distribution of the data was confirmed, a paired *t*-test compared the mean values of the gait parameters, peak values of joint angles and angular velocities, peak values of muscle activity, weighting of muscle synergy, and CoA and FWHM under different conditions. The Friedman test was used to compare the similarity of muscle synergy between the High and Normal conditions (Yaserifar & Oliveira, 2022). In multiple comparison tests, the Wilcoxon test was performed, and the *p*-value was corrected using the Durbin–Conover method. Cohen's d was interpreted as small ($0.2 < d < 0.5$), moderate ($0.5 < d < 0.8$), and large ($d > 0.8$). Statistical analyses were performed using JASP version 0.14.1.0 (JASP Team, 2020), and the significance level was set at 0.05, and a marginally significant was $0.05 \leq p < 1$.

Results

No significant difference was observed in the average stride time, stride length, swing time, stance time, and double support time among the conditions (Table 1).

Qualitatively, the joint angle and angular velocity data were similar between conditions (Fig. 2). No significant difference was observed in the peak values of ankle plantar flexion angle, ankle plantar flexion velocity, and hip flexion velocity during the late stance phase (Table 2).

[Insert Table 1 and Figure 2 about here]

The activity timing of the muscles was qualitatively similar across conditions (Fig. 3). The average cosine similarity between MG and LG under each condition was $r > 0.9$, indicating a highly similar activity pattern between MG and LG (High: $r = 0.90 \pm 0.07$, Normal: $r = 0.90 \pm 0.07$). $P_{MG}^{Late\_stance}$ was significantly higher in the High condition compared with that in the Normal condition, indicating that the experimental conditions were appropriate (Table 2). $P_{RF}^{Late\_stance}$ was significantly lower in the High condition compared with that in the Normal condition (Table 2). $P_{BF}^{Late\_stance}$ was significantly higher in the High condition compared with that in the Normal condition (Table 2).

[Insert Figure 3 and Table 2 about here]

The number of synergies between the High and Normal conditions did not significantly differ (High: 3.5 ± 0.8, Normal: 3.7 ± 0.9, t = 1.5, p = 0.21, d = 0.4). The average r in each muscle synergy between the conditions was >0.70 for both Weighting and Activation (Table 3, Fig. 4), and a high similarity of muscle synergy was observed. However, the similarity between the High and Normal conditions in Synergy-3 was lower than that of other muscle synergies, and a significant difference and a marginally significant were obtained (Table 3, Weighting: χ^2 = 9.2, p = 0.03; Activation: χ^2 = 7.2, p = 0.07). A comparison of CoA and FWHM between conditions showed no significant difference (Table 4).

[Insert Figure 4, Table 3, and Table 4 about here]

Discussion

This study aimed to elucidate the tuning of synergies in muscle activation adjustment of push-off. No significant difference was observed in the number of muscle synergies between the High and Normal conditions, and the similarity of muscle synergies was high (Table 3). Significant differences were observed in the peak muscle activity of MG, RF, and BF between conditions (Table 2). This implies that the muscle synergies during normal walking were maintained, and slight adjustments in the amplitude of muscle activity occurred for each muscle. This is the first demonstration of the muscle activation adjustment mechanism of ankle push-off from the perspective of muscle coordination. The extracted four muscle synergies are referred to as Synergy-1 to -4, respectively (Fig. 4). The characteristics of the extracted muscle synergies were similar to those previously reported (Ivanenko et al., 2004; Kibushi et al., 2018, 2022), suggesting that the extraction method employed in this study was appropriate. Synergy-1 was primarily comprised of the knee extensor (VL), hip flexor (TFL), hip abductor (Gmed), and hip extensor (Gmax) muscles, and its activity was observed immediately following the heel strike, implying that Synergy-1 was involved in the load response. Synergy-2, primarily constituted by the ankle plantar flexors (MG, SOL), exhibited a prominent activity of approximately 40% of the gait cycle, indicating a role in generating propulsion and supporting the body. Synergy-3, primarily comprising the knee extensors (VL, RF), hip flexor (RF), and trunk muscles (ES, EO), showed significant activity before toe-off, suggesting involvement in the acceleration of the swing leg and support of the trunk. Synergy-4, constituted by the ankle dorsiflexor (TA), knee extensor (VL), knee flexor (ST, BF), and hip extensors (ST, BF), displayed a prominent activity just before the subsequent heel strike, implying involvement in the deceleration of the swing leg.

No significant difference was observed in the number of muscle synergies between the High and Normal conditions, and the similarity of muscle synergies was high (Table 3), revealing that even if the MG was adjusted during the push-off, the muscle synergies during normal walking were generally maintained. This result is consistent with those from previous studies that showed that muscle synergies during walking were consistent, providing the walking speed or the combination of stride length and stride time did not significantly change (Kibushi et al., 2018, 2022). In addition, ankle plantar flexion function is enhanced with exoskeletons, and the number of synergies is maintained (Jacobs et al., 2018). In this study, the participants rapidly adapted to increasing MG activity during push-off with 3 min × 2 repetitions of practice. Using existing muscle synergies for motor control has been shown to contribute to rapid adaptation and learning (Al Borno et al., 2020; Berger & D’Avella, 2014; Hagio & Kouzaki, 2018). The rapid adaptation observed in this study may be related to the utilization of existing muscle synergies.

In the present study, I observed changes in the level of individual muscle activity, despite muscle synergy remaining constant. This result is not consistent with previous studies. The control of walking, based on muscle synergy, has been believed to be achieved through four to five distinct muscle synergies (Ivanenko et al., 2004). Adjustments to muscle synergy activity patterns are seen when the walking speed is high (Kibushi et al., 2018) or when the stride length is extremely wide or narrow (Kibushi et al., 2022). However, the extracted muscle synergies in this study did not exhibit significant differences between conditions and were observed individual modulation for RF and BF activation. This suggests that the regulation of muscle activity during walking cannot be solely explained by fine-tuning muscle synergies. While muscle synergy is typically represented by $EMG = WC + residual$, the modulation of RF and BF activation that arises from adjustments in MG activation during the push-off phase might potentially be manifested within the residuals.

Enhancing ankle push-off force enabled compensatory adjustments both during push-off and in the adjacent phases (Lewis & Ferris, 2008; McGibbon & Krebs, 2004). Based on this, I hypothesized that muscle activation adjustment of push-off is performed in the muscle synergy related to ankle push-off and in the muscle synergy that activates during the adjacent push-off phase. However, no significant differences were found in the weighting of muscle synergies, CoA, or FWHM (Table 4), and the hypothesis was not supported. This suggests that muscle activation adjustment of push-off was achieved through adjustments other than via muscle synergies. Synergy-2 may not be adjusted because of a low necessity for increased propulsion and body support. The role of the triceps surae muscles during walking is considered to be required for body support, acceleration of the center of mass forward, and acceleration of the leg swing (Neptune, Kautz, & Zajac, 2001). Thus, Synergy-2, mainly composed of triceps surae muscles, contributes to both body support and propulsion generation, and particularly in high-speed walking, the propulsion originating from the activation of gastrocnemius increases (Liu et al., 2008). In this study, the walking speed was constant. Hence, any additional propulsion or body support may be minimal. If the walking speed increases, Synergy-2 adjustments might be observed.

In this study, although a clear adjustment of muscle synergies could not be confirmed, an adjustment of individual muscles was observed. Under the High conditions, the peak activity of BF increased during the late stance phase while the peak RF activation decreased (Table 2). This adjustment is considered to have been made independently of muscle synergy adjustment. Both ankle plantarflexion torque and knee flexion torque contribute to generating propulsive force during gait (Peterson et al., 2011). Therefore, the increased BF activation during the late stance phase observed in the High condition may have contributed to the generation of additional propulsive force through knee flexion. Furthermore, RF was involved in knee extension during the swing phase, and with decreased activity, knee flexion was observed (Frigo et al., 2020). Reducing the RF activity during the pre-swing phase could reduce interference with knee flexion. Although the quantification of force exertion has not been conducted, the modulation of RF and BF activation could have occurred due to the attempts to help knee flexion.

Synergy-3, which was involved in the pre-swing, exhibited a lower similarity between the High and Normal conditions than that in the other muscle synergies (Table 3). This suggests that Synergy-3 has more adaptability than that in the other extracted muscle synergies. However, no significant difference was observed in the quantitative comparison of weighting and activation (Table 4), and it remains unclear what is being modified. Furthermore, no significant difference was found in hip flexion velocity (Table 2), which implies that modulation in Synergy-3 did not contribute to increasing the leg swing speed. This is likely because the walking speed and cadence were constrained in this study. If changing the walking speed or cadence is allowed, the hip flexion muscle activation might increase.

This study had several limitations. First, the walking parameters were constrained during task execution. Therefore, the effect of enhancement of muscle activation during ankle push-off when accommodating changes in walking speed or stride length remains unknown. Muscle synergies are known to adjust depending on the walking speed and the combination of stride length and stride time (Kibushi et al., 2018, 2022). Consequently, the possibility of muscle synergies being adjusted arises if changes in walking speed and stride length are allowed. Second, the study did not compare kinetic data and it remained unclear whether the enhanced MG activity increased the ankle plantar flexor or hip extension torque. Third, it is unclear whether similar results can be obtained when changing the feedback muscle. The activity of the triceps surae during walking are similar to each other. In this study, the activities of MG and SOL were also similar, and the peak activity of SOL increased in the High condition. Therefore, regardless of which muscle of the triceps surae is used as the feedback target, similar results would be obtained as in this study. Furthermore, it is unknown whether similar results of muscle synergy characteristics can be obtained if other muscle activities, except for the push-off, are evaluated. In future studies, using other subtask-related muscle activity adjustment tasks would reveal the mechanism of adjustment for other subtasks.

Conclusion

This study aimed to elucidate the tuning of muscle synergies in muscle activation adjustment of push-off. No significant difference was observed in the number of synergies and muscle synergy activation (CoA and FWHM) between the

High and Normal conditions. However, the peak muscle activity of MG, RF, and BF did differ between conditions. Muscle synergies during normal walking are therefore maintained, and slight adjustments in the amplitude of muscle activity occurred for each muscle.

Data availability

The datasets analyzed in the current study are available from the corresponding author upon reasonable request.

Conflicts of interest

The authors declare no competing financial interests.

Acknowledgments

This work was supported by the JSPS KAKENHI (Grant number: 21K17627).

Author contributions

Conception and design of the experiments: BK, TM, and MK. Collection, analysis, and interpretation of the data: BK. Drafting the article and critically revising the article for important intellectual content: BK and MK. Final approval of the version to be published: BK, TM, and MK.

References

Aiello, E., Gates, D. H., Patritti, B. L., Cairns, K. D., Meister, M., Clancy, E. A., & Bonato, P. (2005). Visual EMG biofeedback to improve ankle function in hemiparetic gait. *Annual International Conference of the IEEE Engineering in Medicine and Biology - Proceedings*, 7703–7706. https://doi.org/10.1109/IEMBS.2005.1616297

Al Borno, M., Hicks, J. L., & Delp, S. L. (2020). The effects of motor modularity on performance, learning and generalizability in upper-extremity reaching: a computational analysis. *Journal of the Royal Society Interface*, *17*(167).

https://doi.org/10.1098/RSIF.2020.0011

Barroso, F. O., Torricelli, D., Moreno, J. C., Taylor, J., Gomez-Soriano, J., Bravo-Esteban, E., Piazza, S., Santos, C., & Pons, J. L. (2014). Shared muscle synergies in human walking and cycling. *Journal of Neurophysiology*, *112*(8), 1984–1998. https://doi.org/10.1152/jn.00220.2014

Berger, D. J., & D'Avella, A. (2014). Effective force control by muscle synergies. *Frontiers in Computational Neuroscience*, *8*, 46. https://doi.org/10.3389/FNCOM.2014.00046/BIBTEX

Cappellini, G., Ivanenko, Y. P., Poppele, R. E., & Lacquaniti, F. (2006). Motor patterns in human walking and running. *Journal of Neurophysiology*, *95*(6), 3426–3437. https://doi.org/10.1152/jn.00081.2006

Cheung, V. C. K., D'Avella, A., Tresch, M. C., & Bizzi, E. (2005). Central and Sensory Contributions to the Activation and Organization of Muscle Synergies during Natural Motor Behaviors. *Journal of Neuroscience*, *25*(27), 6419–6434. https://doi.org/10.1523/jneurosci.4904-04.2005

Clark, W. H., Pimentel, R. E., & Franz, J. R. (2021). Imaging and Simulation of Inter-muscular Differences in Triceps Surae Contributions to Forward Propulsion During Walking. *Annals of Biomedical Engineering*, *49*(2), 703–715.

Colborne, G. R., Wright, F. V., & Naumann, S. (1994). Feedback of triceps surae EMG in gait of children with cerebral palsy: A controlled study. *Archives of Physical Medicine and Rehabilitation*, *75*(1), 40–45. https://doi.org/10.1016/0003-9993(94)90335-2

DeVita, P., & Hortobagyi, T. (2000). Age causes a redistribution of joint torques and powers during gait. *Journal of Applied Physiology*, *88*(5), 1804–1811. https://doi.org/10.1152/jappl.2000.88.5.1804

Dursun, E., Dursun, N., & Alican, D. (2009). Effects of biofeedback treatment on gait in children with cerebral palsy. *Https://Doi.Org/10.1080/09638280310001629679*, *26*(2), 116–120. https://doi.org/10.1080/09638280310001629679

Esmaeili, S., Karami, H., Baniasad, M., Shojaeefard, M., & Farahmand, F. (2022). The association between motor modules and movement primitives of gait: A muscle and kinematic synergy study. *Journal of Biomechanics*, *134*, 110997. https://doi.org/10.1016/J.JBIOMECH.2022.110997

Franz, J. R., Maletis, M., & Kram, R. (2014). Real-time feedback enhances forward propulsion during walking in old adults. *Clinical Biomechanics*, *29*(1), 68–74. https://doi.org/10.1016/J.CLINBIOMECH.2013.10.018

Frigo, C. A., Wyss, C., & Brunner, R. (2020). The Effects of the Rectus Femoris

Muscle on Knee and Foot Kinematics during the Swing Phase of Normal Walking. *Applied Sciences 2020, Vol. 10, Page 7881*, *10*(21), 7881. https://doi.org/10.3390/APP10217881

Hagio, S., & Kouzaki, M. (2018). Modularity speeds up motor learning by overcoming mechanical bias in musculoskeletal geometry. *Journal of the Royal Society Interface*, *15*(147). https://doi.org/10.1098/RSIF.2018.0249

Hug, F., Turpin, N. A., Guével, A., & Dorel, S. (2010). Is interindividual variability of EMG patterns in trained cyclists related to different muscle synergies? http://www.jap.org. *Journal of Applied Physiology*, *108*(6), 1727–1736. https://doi.org/10.1152/japplphysiol.01305.2009

Ivanenko, Y. P., Poppele, R. E., & Lacquaniti, F. (2004). Five basic muscle activation patterns account for muscle activity during human locomotion. *Journal of Physiology*, *556*(1), 267–282. https://doi.org/10.1113/jphysiol.2003.057174

Jacobs, D. A., Koller, J. R., Steele, K. M., & Ferris, D. P. (2018). Motor modules during adaptation to walking in a powered ankle exoskeleton. *Journal of NeuroEngineering and Rehabilitation*, *15*(1), 1–15. https://doi.org/10.1186/s12984-017-0343-x

JASP Team. (2020). *JASP (Version 0.14) [Computer software]*.

Jonsdottir, J., Cattaneo, D., Regola, A., Crippa, A., Recalcati, M., Rabuffetti, M., Ferrarin, M., & Casiraghi, A. (2007). Concepts of motor learning applied to a rehabilitation protocol using biofeedback to improve gait in a chronic stroke patient: An A-B system study with multiple gait analyses. *Neurorehabilitation and Neural Repair*, *21*(2), 190–194. https://doi.org/10.1177/1545968306290823

Kerrigan, D. C., Todd, M. K., Della Croce, U., Lipsitz, L. A., & Collins, J. J. (1998). Biomechanical gait alterations independent of speed in the healthy elderly: Evidence for specific limiting impairments. *Archives of Physical Medicine and Rehabilitation*, *79*(3), 317–322. https://doi.org/10.1016/S0003-9993(98)90013-2

Kibushi, B., Hagio, S., Moritani, T., & Kouzaki, M. (2018). Speed-dependent modulation of muscle activity based on muscle synergies during treadmill walking. *Frontiers in Human Neuroscience*, *12*, 4. https://doi.org/10.3389/fnhum.2018.00004

Kibushi, B., Moritani, T., & Kouzaki, M. (2022). Modular control of muscle coordination patterns during various stride time and stride length combinations. *Gait & Posture*, *94*, 230–235. https://doi.org/10.1016/J.GAITPOST.2021.04.006

Lee, D. D., & Seung, H. S. (1999). Learning the parts of objects by non-negative matrix factorization. *Nature*, *401*(6755), 788–791. https://doi.org/10.1038/44565

Lewis, C. L., & Ferris, D. P. (2008). Walking with increased ankle pushoff decreases hip muscle moments. *Journal of Biomechanics*, *41*(10), 2082–2089. https://doi.org/10.1016/j.jbiomech.2008.05.013

Lewis, C. L., & Garibay, E. J. (2015). Effect of increased pushoff during gait on hip joint forces. *Journal of Biomechanics*, *48*(1), 181–185. https://doi.org/10.1016/j.jbiomech.2014.10.033

Liu, J., Santucci, V., Eicholtz, S., & Kesar, T. M. (2021). Comparison of the effects of real-time propulsive force versus limb angle gait biofeedback on gait biomechanics. *Gait & Posture*, *83*, 107–113. https://doi.org/10.1016/J.GAITPOST.2020.10.014

Liu, M. Q., Anderson, F. C., Schwartz, M. H., & Delp, S. L. (2008). Muscle contributions to support and progression over a range of walking speeds. *Journal of Biomechanics*, *41*(15), 3243–3252. https://doi.org/10.1016/J.JBIOMECH.2008.07.031

McGibbon, C. A., & Krebs, D. E. (2004). Discriminating age and disability effects in locomotion: Neuromuscular adaptations in musculoskeletal pathology. *Journal of Applied Physiology*, *96*(1), 149–160. https://doi.org/10.1152/JAPPLPHYSIOL.00422.2003/ASSET/IMAGES/LARGE/DG0142796003.JPEG

Neptune, R. R., Clark, D. J., & Kautz, S. A. (2009). Modular control of human walking: A simulation study. *Journal of Biomechanics*, *42*(9), 1282–1287. https://doi.org/10.1016/j.jbiomech.2009.03.009

Neptune, R. R., Kautz, S. A., & Zajac, F. E. (2001). Contributions of the individual ankle plantar flexors to support, forward progression and swing initiation during walking. *Journal of Biomechanics*, *34*(11), 1387–1398. https://doi.org/10.1016/S0021-9290(01)00105-1

Neptune, R. R., & Sasaki, K. (2005). Ankle plantar flexor force production is an important determinant of the preferred walk-to-run transition speed. *Journal of Experimental Biology*, *208*(5), 799–808. https://doi.org/10.1242/jeb.01435

Peterson, C. L., Kautz, S. A., & Neptune, R. R. (2011). Braking and propulsive impulses increase with speed during accelerated and decelerated walking. *Gait & Posture*, *33*(4), 562–567. https://doi.org/10.1016/J.GAITPOST.2011.01.010

Santuz, A., Ekizos, A., Eckardt, N., Kibele, A., & Arampatzis, A. (2018). Challenging human locomotion: Stability and modular organisation in unsteady conditions. *Scientific Reports*, *8*(1), 1–13. https://doi.org/10.1038/s41598-018-21018-4

Sawers, A., Allen, J. L., & Ting, L. H. (2015). Long-term training modifies the modular structure and organization of walking balance control. *Journal of Neurophysiology*, *114*(6), 3359–3373. https://doi.org/10.1152/jn.00758.2015

Torres-Oviedo, G., Macpherson, J. M., & Ting, L. H. (2006). Muscle Synergy Organization Is Robust Across a Variety of Postural Perturbations. *Journal of Neurophysiology*, *96*(3), 1530–1546. https://doi.org/10.1152/jn.00810.2005

Torres-Oviedo, G., & Ting, L. H. (2007). Muscle synergies characterizing human postural responses. *Journal of Neurophysiology*, *98*(4), 2144–2156. https://doi.org/10.1152/jn.01360.2006

Tresch, M. C., Saltiel, P., & Bizzi, E. (1999). The construction of movement by the spinal cord. *Nature Neuroscience*, *2*(2), 162–167. https://doi.org/10.1038/5721

Yaserifar, M., & Oliveira, A. S. (2022). Inter-muscular coordination during running on grass, concrete and treadmill. *European Journal of Applied Physiology*, *3*, 1–12. https://doi.org/10.1007/S00421-022-05083-2/FIGURES/5

Zelik, K. E., & Adamczyk, P. G. (2016). A unified perspective on ankle push-off in human walking. *Journal of Experimental Biology*, *219*(23), 3676–3683. https://doi.org/10.1242/jeb.140376

Figure legends

Figure 1: Experimental setup.

The participants adjusted the current waveform with the target waveform displayed on a monitor located 1.5 m ahead. The current waveform is shown in yellow, and white lines represent the target waveform. The current waveform was updated every cycle. The ensemble-averaged MG was generated by normalizing MG activity by the maximum value during normal walking and averaging it over 30 cycles. Target waveforms were output by multiplying the scaling factor (High = 1.6, Low = 0.4) by the ensemble-averaged MG. The scaling factors were explored in a preliminary experiment. In these scaling factors, participants could increase or decrease muscle activity as much as possible without fatigue.

Figure 2: Ensemble averages of joint angle (A–C) and angular velocity (D–F) among participants.

The zero degrees were defined as the anatomical position. Red and blue waveforms represent ensemble averages in High and Normal conditions. The deviation of data was demonstrated as the box plot at each time point in every 5% of the gait cycle. Circles and horizontal black lines indicate outliers and median, respectively. The bottom and upper edges of the box represent the first and third quartiles, respectively. The upper and bottom edges of vertical lines represent maximum and minimum values, respectively. The vertical dotted line represents the right toe-off.

Figure 3: Ensemble averages of EMG among participants.

Red and blue waveforms represent ensemble averages in High and Normal conditions. The deviation of data was demonstrated as the box plot at each time point in every 5% of the gait cycle. Circles and horizontal black lines indicate outliers and median, respectively. The bottom and upper edges of the box represent the first and third quartiles, respectively. The upper and bottom edges of vertical lines represent maximum and minimum values, respectively. The vertical dotted line represents the right toe-off. Abbreviations: gastrocnemius medialis (MG), soleus (SOL), rectus femoris (RF), biceps femoris (BF).

Figure 4: Weightings (A, C, E, G) and ensemble average activation (B, D, F, H) of the muscle synergies.

The average weightings of the muscle synergies are represented as bars. White bars denote no significant muscle weighting (lower bound of the 95% CI was smaller than zero). The ensemble average activation levels are represented as waveforms. The deviation of data was demonstrated as the box plot at each time point in every 5% of the gait cycle. Circles and horizontal black lines indicate outliers and median, respectively. The bottom and upper edges of the box represent the first and third quartiles, respectively. The upper and bottom edges of vertical lines represent maximum and minimum values, respectively. The vertical dotted line represents the right toe-off. Red and blue bars/waveforms represent ensemble averages in High and Normal conditions. Cosine similarity values between the conditions are indicated on the left upper side of each bar and waveform. Abbreviations: gastrocnemius medialis (MG), soleus (SOL), tibialis anterior (TA), vastus lateralis (VL), rectus femoris (RF), biceps femoris (BF), semitendinosus (ST), tensor fasciae latae (TFL), gluteus medius (Gmed), gluteus maximus (Gmax), erector spinae at L5 (ES), and abdominal external oblique (EO).

Table 1: Average gait parameters among participants.

Table 2: Peak values of joint angle, angular velocity, and EMG amplitude.

Significant differences are emphasized in bold. Peak values were calculated during the late stance phase (30–60% of gait cycle). $P_{Ank-plant-deg}^{Late-stance}$: ankle plantar flexion degree, $P_{Ank-plant-vel}^{Late-stance}$: ankle plantar flexion velocity, $P_{Hip-flex-vel}^{Late-stance}$: hip flexion velocity, $P_{MG}^{Late-stance}$: gastrocnemius medialis, $P_{RF}^{Late-stance}$: rectus femoris, $P_{BF}^{Late-stance}$: biceps femoris.

Table 3: Average cosine similarities (r) between conditions.

The *t*-value and *p*-value are the results of a multiple comparison test regarding the difference in similarity between Synergy-3 and other muscle synergies. The correction of *p*-value using the Durbin-Conover method was conducted after the Wilcoxon test. Significant differences are emphasized in bold.

Table 4: Average CoA and FWHM among participants.

The CoA represents the temporal duration of the gait cycle (0–100%) as an angle (0–360°). Zero degrees signify the ground contact, with the progression of time corresponding to an increase in the angle. Negative values indicate instances before ground contact.

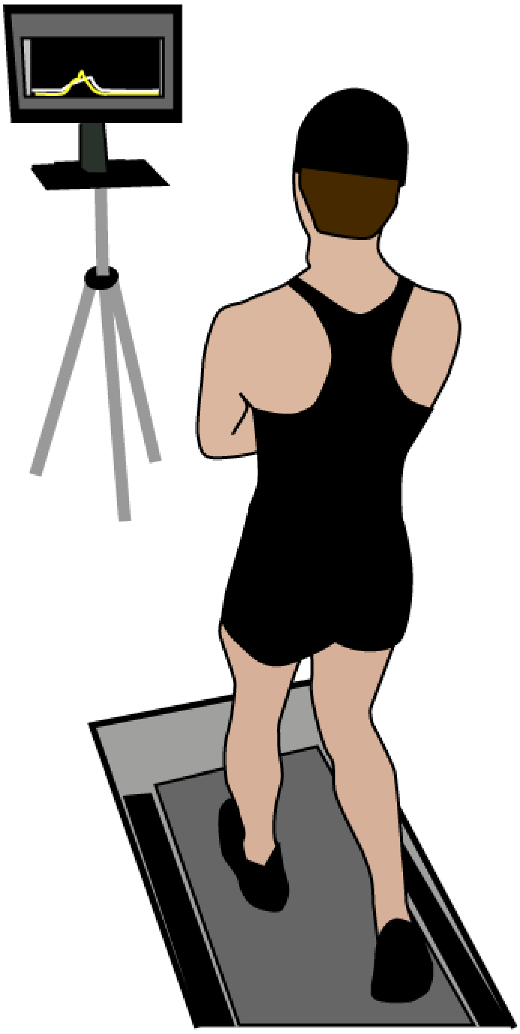

Figure 1

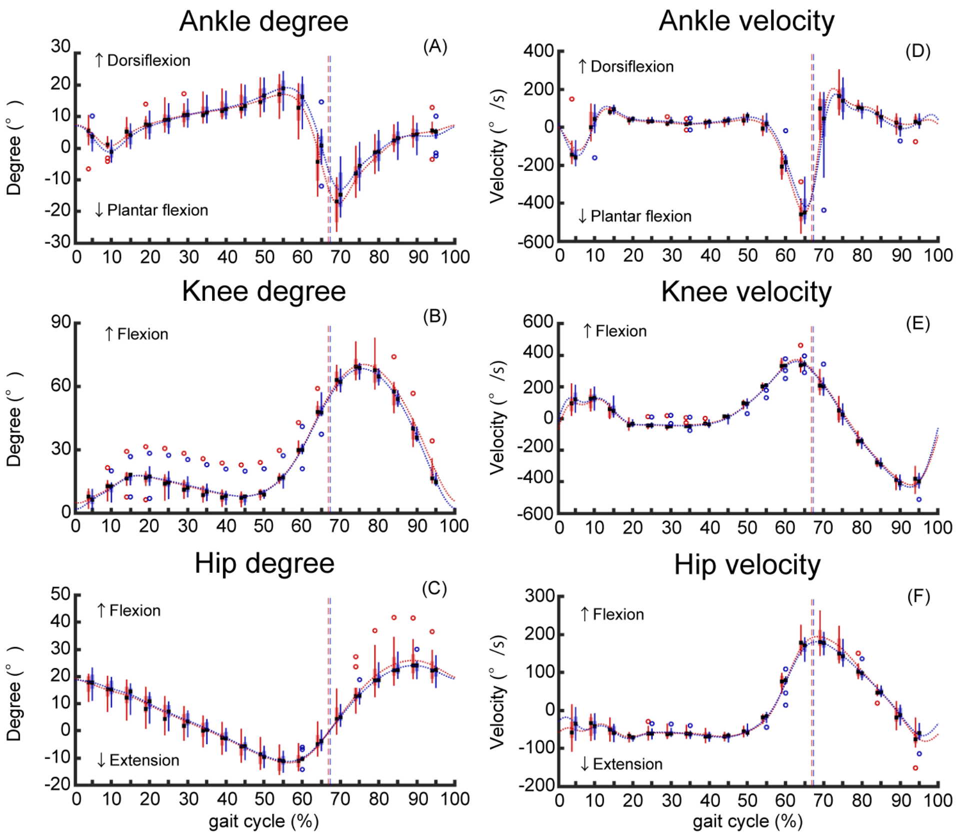
Ankle degree
(A)
↑ Dorsiflexion
↓ Plantar flexion
Degree (°)
Ankle velocity
(D)
↑ Dorsiflexion
↓ Plantar flexion
Velocity (° /s)
Knee degree
(B)
↑ Flexion
Degree (°)
Knee velocity
(E)
↑ Flexion
Velocity (° /s)
Hip degree
(C)
↑ Flexion
↓ Extension
Degree (°)
gait cycle (%)
Hip velocity
(F)
↑ Flexion
↓ Extension
Velocity (° /s)
gait cycle (%)

Figure 2

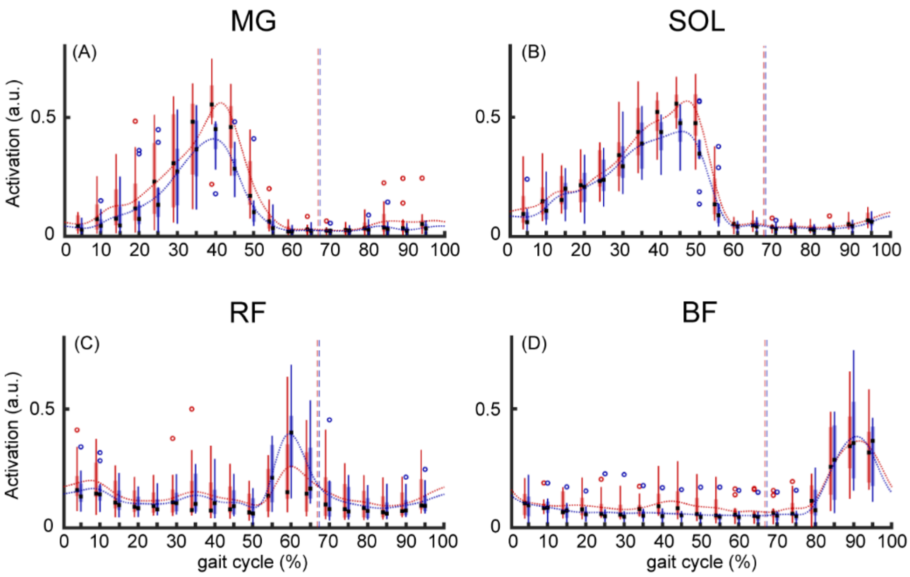
MG
SOL
RF
BF
(A)
(B)
(C)
(D)
Activation (a.u.)
gait cycle (%)
0
0.5
0 10 20 30 40 50 60 70 80 90 100

Figure 3

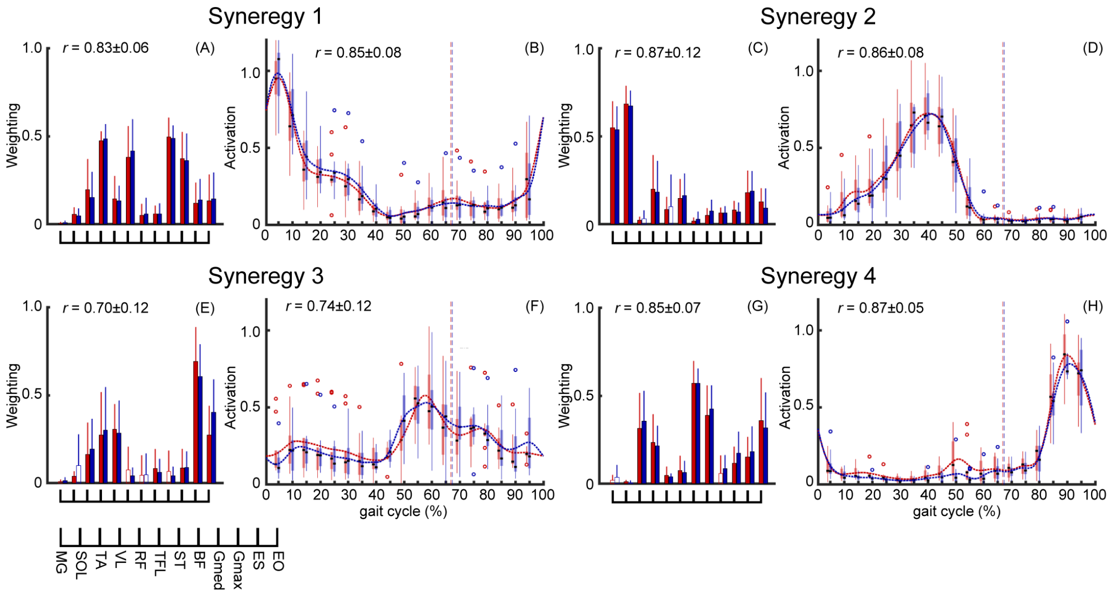

Syneregy 1
Syneregy 2
Syneregy 3
Syneregy 4
r = 0.83±0.06
(A)
r = 0.85±0.08
(B)
r = 0.87±0.12
(C)
r = 0.86±0.08
(D)
r = 0.70±0.12
(E)
r = 0.74±0.12
(F)
r = 0.85±0.07
(G)
r = 0.87±0.05
(H)
Weighting
Activation
gait cycle (%)
MG
SOL
TA
VL
RF
TFL
ST
BF
Gmed
Gmax
ES
EO

Figure 4

	High	*Normal*	*t-value*	*p-value*	*Cohen's d*
Speed (m/s)	1.25	1.25	-	-	-
Stride time (s)	1.0 ± 0.0	1.0 ± 0.0	1.7	0.12	0.51
Stride length (m)	1.25 ± 0.0	1.25 ± 0.0	1.7	0.12	0.51
Stance time (s)	0.67 ± 0.01	0.67 ± 0.02	1.7	0.11	0.52
Swing time (s)	0.33 ± 0.01	0.33 ± 0.02	1.7	0.13	0.50
Double support time (s)	0.16 ± 0.01	0.17 ± 0.01	0.7	0.50	0.22

Table 1

	High	*Normal*	*t-value*	*p-value*	*Cohen's d*
$P_{Ank-plant-deg}^{Late-stance}$ (°)	-18.4 ± 5.8	-14.9 ± 5.6	2.2	0.05	0.67
$P_{Ank-plant-vel}^{Late-stance}$ (°/s)	-480.7 ± 72.7	-467.3 ± 69.9	0.8	0.42	0.25
$P_{Hip-flex-vel}^{Late-stance}$ (°/s)	200.2 ± 34.7	186.4 ± 15.1	1.5	0.15	0.47
$\boldsymbol{P_{MG}^{Late-stance}}$ **(a. u.)**	**0.66 ± 0.13**	**0.50 ± 0.12**	**8.4**	**< 0.01**	**2.54**
$\boldsymbol{P_{RF}^{Late-stance}}$ **(a. u.)**	**0.32 ± 0.21**	**0.45 ± 0.17**	**2.9**	**0.02**	**0.87**
$\boldsymbol{P_{BF}^{Late-stance}}$ **(a. u.)**	**0.16 ± 0.01**	**0.08 ± 0.06**	**2.9**	**0.02**	**0.86**

Table 2

		r	*t-value*	*p-value*
Weighting	**Synergy-1**	**0.83 ± 0.06**	**2.1**	**< 0.05**
	Synergy-2	**0.87 ± 0.12**	**2.9**	**0.01**
	Synergy-3	0.70 ± 0.12	-	-
	Synergy-4	0.85 ± 0.07	1.9	0.07
Activation	Synergy-1	0.85 ± 0.08	1.5	0.14
	Synergy-2	**0.86 ± 0.08**	**2.3**	**0.03**
	Synergy-3	0.74 ± 0.12	-	-
	Synergy-4	**0.87 ± 0.06**	**2.3**	**0.03**

Table 3

		High	*Normal*	*t-value*	*p-value*	*Cohen's d*
CoA (°)	Synergy-1	26.0 ± 23.6	30.1 ± 20.9	0.6	0.47	0.22
	Synergy-2	128.1 ± 10.5	130.6 ± 15.3	0.7	0.52	0.22
	Synergy-3	177.6 ± 100.2	189.2 ± 98.8	1.2	0.27	0.43
	Synergy-4	-42.7 ± 17.6	-37.6 ± 8.5	0.6	0.59	0.19
FWHM (%)	Synergy-1	15.4 ± 3.8	17.7 ± 5.9	0.1	0.92	0.03
	Synergy-2	25.4 ± 8.4	23.2 ± 6.0	0.6	0.59	0.17
	Synergy-3	28.0 ± 20.6	31.6 ± 18.3	0.7	0.48	0.22
	Synergy-4	14.0 ± 6.1	14.2 ± 5.7	0.3	0.78	0.09

Table 4